



## Determination of Rock Thermal Conductivity Under in-Situ Conditions: Experimental and Numerical Investigation

---

Hem Bahadur Motra, Frederick Sittig, Dennis Schwindrofska,  
Amir Shoarian Sattari and Frank Wuttke

EasyChair preprints are intended for rapid  
dissemination of research results and are  
integrated with the rest of EasyChair.

May 23, 2020

# Determination of rock thermal conductivity under in-situ conditions: Experimental and numerical investigation

Motra Hem Bahadur\*, Sittig Frederick, Schwindrofska Dennis, Sattari Amir Shoarian and Wuttke Frank

University of Kiel, Department of Geoscience, Geomechanics and Geotechnics, Kiel Germany

**Abstract.** In this study, the effects of pressure and temperature on thermal conductivity of natural mono-minerals rocks in in-situ condition is investigated. Heat transfer in rock masses is one of the most critical crucial processes that needs to be considered in subsurface engineering applications, such as radioactive waste repositories, geothermal energy, and oil and gas storages. Despite the need, there is no direct method for measuring the change of thermal conductivity under high pressure and temperature loadings similar to what is found in in-situ condition. Therefore, in this study the thermal conductivity of 5 mono-mineral rock samples (Anhydrit, Mormor, Quarzit, Gips, Obsidan/perlit) under in-situ conditions are determined during a steady state and while using a reference material for direct measurement of thermal conductivity. The measurements are made over a temperature and hydrostatic pressure range of room temperature to 400 °C and 12 MPa to 400 MPa, respectively. The results indicate that the thermal conductivity of all samples increase with increasing pressure. The non-linear increase of thermal conductivity is found for rock samples at low hydrostatic pressure below 100 MPa. Additionally, the effect of micro-structure and mineralogical composition on thermal conductivity of mono-minerals rocks is discussed. The test results constitute the first systematic measurement of thermal conductivity on in-situ condition of different type of rocks and can be further used for the development of thermal models for predicting the thermal responses.

## 1 Introduction

Thermal conductivity is one of the key properties for geothermal heat flow studies and is also vital for other applications, like petroleum geology, application of geothermal energy, civil engineering application, and hydrogeological application [1]. In the earth's lithosphere, conduction of heat generally dominates among the others mechanisms as radiation and advection. In order to make estimates of crustal temperature from heat flow and geothermal gradient, it's necessary to have information regarding the thermal conductivity of crustal layers and its dependence of pressure and temperature is necessary [2].

Thermal conductivity is a physical property of materials which quantifies the ability of the material to transport heat through the body itself. For conduction, the transfer of heat is due to molecular activity, causing molecules in hotter regions to exchange their kinetic and vibrational energies with adjacent molecules through random motion and collisions. In the last 50 years, a large number of different measuring methods have been developed and applied for determining the thermal conductivities of rocks. These methods typically have different criteria for the sample geometry, the temporal regime and spatial distribution of the temperature and pressure field, i.e. the initial boundary conditions, which must also be taken into account when solving the heat

conduction equation. But still lacking of measuring thermal conductivity of rock in in-situ boundary conditions. However, the measurement of thermal conductivity at high pressure and temperature is still lacking.

Numerous measurements of thermal properties are done at high pressure but at room temperature, or at high temperature and low pressure, or at room temperature and atmospheric pressure. There are numerous steady state "divided bar-methods" [3, 4] and transient line-source "needle probe" techniques [4, 5] that are available for measuring thermal conductivity and follow Fourier's heat transfer theory. The most prominent being the divided bar and the needle probe method. These methods are discussed in detail in several books and journal contributions [6, 7]. A similar method is the application of the guarded hot plate device to determine the thermal conductivity. This method in particular is highly accurate and well developed. However, the application of in-situ stresses is not seen in current technical solutions [8]. More sophisticated technical solutions for thermal flux have been designed by Lambda Measurement Consulting, but these solutions were devised without the use of any cell pressure. Other methods developed by [9] are the "optical thermal conductivity scanner" and the "laser flash method". These methods were developed to measure thermal diffusivity and both provide additional information about the dependence of

---

\* Corresponding author: hem.motra@ifg.uni-kiel.de

mineralogy heterogeneity in relation to thermal conductivity. However, neither are applicable for samples which undergo high overburden pressure. Heat transfer in solids with an ordered crystal structure have a wave like nature, which is described by [10, 11]. Parameters such as texture, bulk density and water content of soil are the key factors, which influence thermal conductivity [12]. Despite the need, there is no existing method for the measuring thermal conductivity at both high pressures and temperatures or in-situ condition for rock material. The goal of this work is not only to measure the pressure- and temperature-dependent thermal conductivities of rocks, but also to develop the simulation model in the same boundary conditions of the measurement and obtained physical processes to the micro level of the samples.

## 2 Method

### 2.1 Steady heat conduction

We have applied a one-dimensional steady state heat flow method to determine the thermal conductivity of the rock sample as a function of pressure and temperature with the help of reference materials (specific high load and temperature resistant ceramic plate ZRO2-Y-PSZ). Steady state methods apply a one-directional heat flow through a specimen and then observe power or temperature differences across the sample when a steady state condition has been reached. The thermal conductivity of the specimen is then obtained using Fourier's Law. Generally, steady state techniques are helpful when the temperature of the specimen does not change with time, these are deemed to be more accurate than transient techniques of thermal conductivity determination. However, the main limitation of steady state methods is that it is dependent on a well-engineered experimental setup as well as ample time for establishing a steady state condition. A steady state thermal conductivity and diffusivity meter which works on the principle of the divided bar apparatus technique. The mathematical description of the one-dimensional conductive heat transport within the device is found using Fourier's law and the conservation of energy. According to Fourier's law, the rate of heat flow of heat energy per unit area through a surface is proportional to the negative temperature gradient across the surface. The heat flux  $q$  (generated by the temperature gradient created due to the heating  $T_1$  and cooling plates  $T_3$ ) through the specimen can be expressed in terms of the thermal conductivity  $\lambda$  as :

$$q = -\lambda \nabla T = -\lambda \frac{\Delta T}{\Delta S} = -\frac{\Delta T}{\Delta S / \lambda} \quad (1)$$

Where,  $S$  is the vertical distance between the respective temperature gradient points across the central axis of the device (Fig. 1). Under the steady state heat flow conditions, provided that  $T_1 > T_2 > T_3$  (heat flow from  $T_1$

top of sample to reference plate  $T_3$  as a liner temperature gradient over height of sample). Equation 1 can be deduced using eqs. 2 and 3 for heat flux between thermal sensor  $T_2$  and  $T_3$  and between sensors  $T_1$  and  $T_3$ , respectively.  $\lambda_V$  is the known thermal conductivity of reference plate.

$$q = -\frac{T_2 - T_3}{S_{23} / \lambda_V} \quad (2)$$

$$q = -\frac{T_1 - T_3}{\frac{S_R}{\lambda_R} + \frac{S_P}{\lambda_S}} \quad (3)$$

$$\lambda_S = \frac{\lambda_R S_P}{\left[ \frac{T_1 - T_3}{T_2 - T_3} \right] S_{23} - S_R} \quad (4)$$

Where,  $T_1$ ,  $T_2$  and  $T_3$  are the temperature of the top heating side of the sample, reference plate and bottom cooling side of reference plate,  $\lambda_S$  and  $\lambda_R$  ( $Wm^{-1}K^{-1}$ ) are the thermal conductivities of rock sample and reference plate,  $S_P$ ,  $S_R$ ,  $S_{23}$  are the distance as shown in Fig. 1.

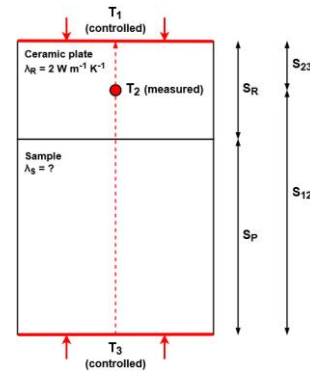


Fig. 1 : Dimensional analysis of the thermal conductivity measurement

### 2.2 Experimental apparatus and rock samples

The multi-anvil pressure apparatus (Fig.3) has been used to measure the thermal conductivity of our rock samples. This device allows for the measurements of elastic wave velocities ( $V_p$ ,  $V_s$ ) and volume (density) change of rocks and thermal conductivity at confining pressure, deviatoric stress and temperature. Measurements can be done simultaneously in three orthogonal directions of a sample cube (43 mm on edges) over a range of pressures up to 600 MPa and temperatures up to 600°C, and using the ultrasonic pulse transmission technique. For thermal conductivity measurement we added one extra thermos element sensor which is shown in Fig. 2 which the heat will allow to flow one axial and other side of sample is completely covered by isolation material which is reduce

to heat loss from other direction. The data are important for geophysical, geotechnical, geothermal modelling and for civil Engineering.

The five monomineral samples (Anhydrit, Mormor, Quarzit, Gips, Obsidan/perlit) (see Fig. 2) are tested to measure the thermal conductivity. A steel sample is used for calibration of thermal conductivity and heat flow.

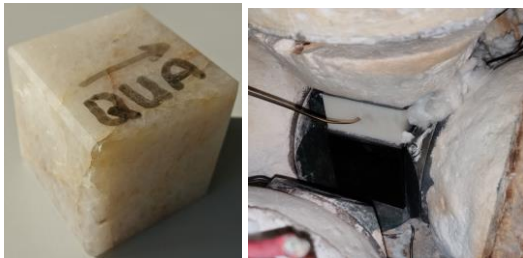


Fig. 2: Quart sample and Steady state thermal conductivity measurement set-up

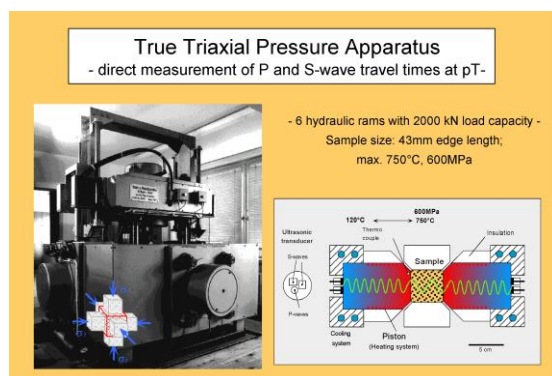


Fig 3: True-triaxial multi-anvil press used to measure thermal conductivity of rock samples.

### 3 Effective thermal conductivity of heterogeneous mono-mineral rocks

#### 3.1 Experimental results

In order to measure the thermal conductivity, a steady state heat flow method is applied and all data are measured under dry condition with respect to as a function of pressure and temperature. The five monomineral (Anhydrit, Mormor, Quarzit, Gips, Obsidan/perlit) samples contained open and interconnected pores with random orientation.

The measurement results of effective thermal conductivity for the five dry mono minerals rocks are reported in Table 1. Temperature dependence was measured from 300K to 673K at 50K or 100 K interval and pressure dependence from 12 MPa to 300 MPa for the quart sample. All detailed results are presented in Table 1 and quart sample results are presented in Fig 4 and 5.

#### 3.1. Effect of pressure on thermal conductivity of rocks

The effect of pressure on effective thermal conductivity is smaller than effect of temperature in all boundary conditions of measurement. From the beginning to approximately 150 MPa pressure the thermal conductivity was increasing nonlinearly with the increase of pressure. From 150 MPa pressure, the thermal conductivity increased in all samples, but in a linear fashion. At high pressures when all of the cracks are assumed to be closed, additional pressure increase does not change the thermal conductivity (see. Fig 4).

#### 3.1. Effect of temperature on thermal conductivity of rocks

Temperature significantly affects the thermal conductivity of rocks. When temperature increase, the thermal conductivity significantly decreases in all of the rock samples. The thermal stress increase with temperature and cracking may create new cracks between the mineral grains as well as expand pre-existing cracks. Therefore, the thermal conductivity decreases with the increase of thermal stress. The nature of decreasing for all five mono-minerals rocks are similar.

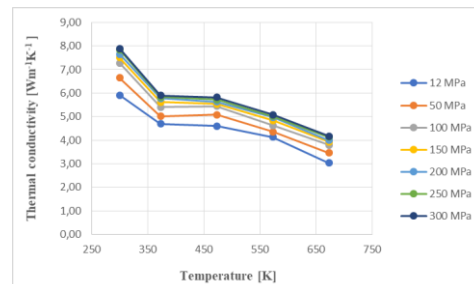


Fig 4: Experimental thermal conductivity of quart sample a a function temperature with different constant pressure

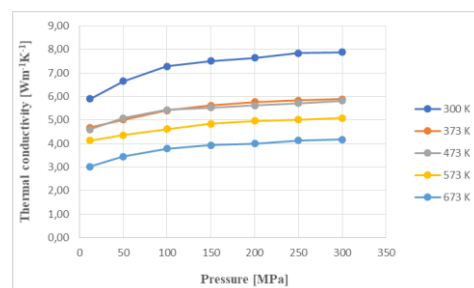


Fig 5: Experimental thermal conductivity of quart sample a a function of pressure with different constant temperature

#### 3.3 Numerical modelling

The finite element analysis was executed by the software Abaqus 6.14. In the very first step, the single parts (sample and ceramic) that are required for the model must be created. After assigning the respective properties, the two parts are assembled (see Fig 6). Since

the interactions between the sample and the ceramic plate are neglectable, the two parts are merged into a stack, but the different properties are retained. The units of the properties are defined uniformly by the International System of Units (SI). The following properties and respective units are used in this simulation: density [ $\text{kg m}^{-3}$ ], Young's modulus [Pa], Poisson ratio [-], heat conductivity [ $\text{W m}^{-1} \text{K}^{-1}$ ] and the specific heat capacity [ $\text{J K}^{-1} \text{kg}^{-1}$ ]. The whole stack can be considered as a continuum, since the porosity of the samples is very low. In regards to the smaller surface area of the pistons compared to that of the sample, the creation of partition faces is inevitable. The different stress loads will be applied over the partition faces. In a subsequent step, six reference points for each piston of the multi-anvil pressure apparatus are generated and constrained with the respective partition face. Here the coupling constraints must be chosen to ensure that one reference point is effective for all points of the respective partition face. For analyzing the model, the process is divided into three steps.

The initial step is set by default and contains all the information of the model before the load is applied. Due to the structural analysis and heat transfer two more steps are required: The first one applies the pressure [Pa] and the second one applies the temperature [K]. The confining pressure is applied over the load module with uniform distribution on the partition faces, whereas the temperature is set via boundary conditions in the interaction module.

The types of the steps are called “coupled temperature-displacement” for combining the structural analysis and the heat transfer. Additionally, the boundary conditions must be defined. Every reference point is also used as a boundary condition. For each step the boundary conditions must be modified. When the boundary conditions are defined for the initial step, they must be modified in the following steps. By choosing the type of “displacement/rotation” and by constraining all degrees of freedom in the initial step, the model is kept in the same position during the test. For the following two steps, the modification of the boundary conditions enables the model to react to the applied loads, e.g. that possible deformation takes place along the edges between the partition faces.

Before starting the analysis, the mesh must be generated. The mesh type used in this simulation is a three-dimensional free mesh (see Fig 8), consisting of 75053

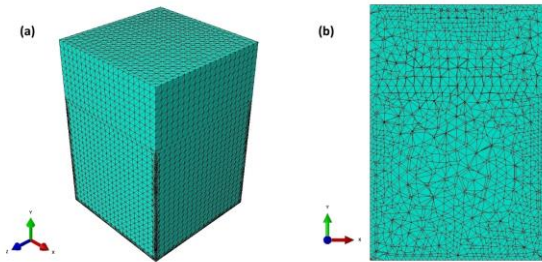


Fig 6: The mesh used for this simulation. (a) shows the tetrahedral mesh over the body surface. The darker regions along the cube edges symbolize the refinement due to displacement. (b) displays a view cut along the z-axis. Here the free and unstructured meshing technique can be seen clearly.

tetrahedral elements and 15471 nodal points. Due to the free meshing technique the meshing type is unstructured, hence the pattern of connectivity is not periodic, and the number of elements connected to a node is unpredictable. Abaqus labels the mesh as “C3D4T” which means that each element is a 4-node thermally coupled tetrahedron with linear displacement and temperature. For the basic model, there is a node every 0.00215 m (e.g. a 20th of the lengths of the cube). Since most of the displacement takes place between the partition faces, the mesh needs to be refined. For these regions, the distance between the nodes is 0.00043 m (e.g. a 100th of the lengths of the cube). Once modelled the experiment, the higher mesh density ensures adequate results.

Since Abaqus is not able to model the thermal conductivity directly,  $\lambda$  is calculated over the heat flux  $q$  [ $\text{W m}^{-2}$ ]. For this purpose, an element set is generated in the center of the sample cube. By adding a new history output, the heat flux can be modelled for this single element. The input properties are pressure and temperature dependent. The modelled thermal conductivity  $\lambda_s$  is calculated over the heat flux  $q$  by rearranging Equation 5.

$$\lambda_s = \frac{q}{\frac{\delta T}{\delta x}} \quad (5)$$

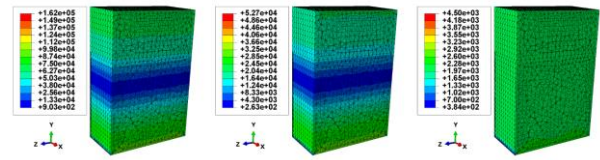


Fig 7: left: after 90 s, middle: after 230 s and right: after 1700 s

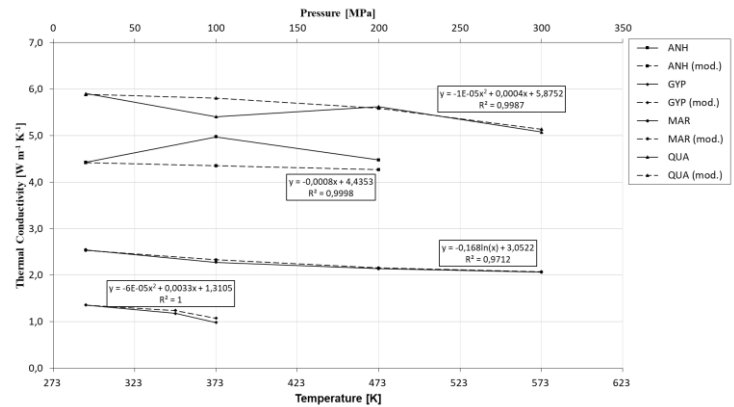


Fig 8: Comparison of thermal conductivity (experimental and numerical results)

The result of thermal conductivity obtained from the numerical heat flow are shown in Fig. 8 and Table 1. As shown in Fig. 8 and Table 1, we calculated the thermal

conductivity with the help of one axial heat flow numerical simulation. It should be pointed out the presented values are the average value of thermal conductivity for entire samples. When comparing the results of the numerical simulation and the measured value of thermal conductivity, we find the following: during the experimental measurement in the laboratory we lose some amount of heat in lateral heat flow direction but we can completely prevent numerical analysis. The difference between simulated and measured thermal conductivity is quite small. However, the different averaging values not only agree well but are also our difference within the tolerance limit.

Table 1: Experimental and numerical analysis results

Pressure [MPa]	Temperature [K]	$\lambda_{e,n}$ [ $W m^{-1} K^{-1}$ ]		Deviation [%]
		experimental	numerical	
<b>STEEL</b>				
12	313	15.25	15.28	+ 0.20
100	373	17.82	17.97	+ 0.84
200	473	24.29	23.61	- 2.80
300	573	26.59	26.30	- 1.10
<b>ANHYDRITE</b>				
12	313	4.42	4.42	0
100	373	4.97	4.35	- 12.47
200	473	4.48	4.27	- 4.69
<b>GYPSUM</b>				
12	313	1.36	1.35	- 0.74
75	348	1.18	1.24	+ 5.08
100	373	0.98	1.07	+ 9.18
<b>MARBLE</b>				
12	313	2.54	2.53	- 0.40
100	373	2.28	2.33	+ 2.19
200	473	2.14	2.15	+ 0.47
300	573	2.06	2.07	+ 0.49
<b>PERLITE</b>				
12	313	0.70	0.73	+ 4.29
100	373	1.81	1.59	- 12.15
200	473	2.53	2.44	- 3.56
300	573	3.12	3.05	- 2.24
<b>QUARTZITE</b>				
12	313	5.90	5.89	- 0.17
100	373	5.41	5.81	+ 7.39
200	473	5.62	5.59	- 0.53
300	573	5.08	5.14	+ 1.18

#### 4 Discussion and conclusion

This work combines laboratory measurement on heterogeneous five mono minerals rock samples and numerical modelling of thermal conductivity. The determination of thermal conductivity as a function of pressure and temperature (in-situ conditions) is the first time that experimental results have been verified with a numerical approach.

Steady-state methods of thermal conductivity measurement are generally the most reliable and offer

relative ease in simulating subsurface conditions of pressure and temperature.

The combined effect of both pressure and temperature on the thermal conductivity is sample-specific and depicted in Figures 4, 5 and 8 and as well Table 1. For the crystalline rocks, the two applied forces act in contradiction to each other. In contrast to that,  $\lambda$  is influenced by pressure and temperature in an enhanced increase for amorphous solids or non-porous materials. As a general trend,  $\lambda$  is decreasing for the crystalline rock samples. Hence, the effect of the temperature is significantly more distinct than the effect of the pressure. Even though the samples experience a pressure-dependent increase in  $\lambda$ , the total alteration of  $\lambda$  is negative. Anhydrite does not fit into this trend, but its thermal conductivities seem to be measured too high at 373 K, 100 MPa and 473 K, 200 MPa. Another error in measurement is obtained for quartzite at 373 K, 100 MPa where  $\lambda$  is measured too low. Despite this error, it can be stated that quartzite has the most striking loss of  $\lambda$  as it is almost divided by a factor of 2. Even though the initial value is nearly halved, the  $\lambda$  at the end of the tests are still greater than the majority of rocks or rock-forming minerals. Hence, the amount of quartzite within a sample plays an important role for estimating the total thermal conductivity of quartz-containing rocks. At temperatures of up to 773 K its temperature-dependent decrease in the thermal conductivity can fall to one third of the value at standard conditions [2]. Due to the sample's low porosities, less voids which could be closed with pressure exist. This is supported by the fact that the temperature-induced decrease is constantly greater than the pressure-induced increase. Additionally, even closed cracks could act as scattering centers for the heat carrying phonon [1]. For perlite and the steel sample, this phenomenon has a much smaller effect due to their amorphous or non-porous fabric. Thus, their lattice thermal conductivity is enhanced with both increasing pressure and increasing temperature due to the nearly undisturbed propagation of the phonons.

The modelled  $\lambda_n$  are in a notably close agreement with the experimental  $\lambda_e$  with a maximum deviation of less than 13 %. Previous performed tests on the pressure- and temperature-dependent behavior of the physical properties, like density or the thermal conductivity itself, are inevitable.

By means of steady state method using True-triaxial multi-anvil press the thermal conductivity, pressure and temperature relationship for five mono-mineral samples are measured and experimental results were validated with numerical simulation. The experimental results fit with the numerical simulation results for the one-axial heat flow for all five rock samples.

The pressure and temperature effect on thermal conductivity strongly depends on the nature of the rock, from mineralogical composition, porosity, density, micro-crack and crack on the rock samples. Therefore, we concluded that the thermal conductivity of dry rock has been shown as the function of density, porosity, grain size and shape, mineral composition as well as micro cracks. In general, we found that the thermal conductivity of rock increases with the increases of

pressure. This would be expected since the increase of overall density of the rock improves the thermal contact between mineral grains, increase the overall density of the rock and consequently, increase the thermal conductivity of the dry rock. On the other hand, for thermal conductivity we found decrease with increased temperature. That means that thermal conductivity should vary with the reciprocal of temperature.

The multi-anvil pressure apparatus that was utilized is able to measure the acoustic characteristics and the thermal conductivities due to the pulse emission technique and the steady-state divided bar method, respectively. Both techniques are very time-consuming which limits the amount of experiments for this work drastically. Every measurement of each sample was carried out once. Additionally, it turns out that a one-directional heat flow for the thermal conductivities was insufficient for this experimental setup. According to the comparison with the simulations, this setup change is not as grievous as it was expected.

The measured values of thermal conductivity of dry rocks were used to confirm the applicability of theoretical and numerical models.

## References

1. Z. Abdulagatova, I. Abdulagatova, V. Emirov, International Journal of Rock Mechanics and Mining Sciences 46, 1055– 107 (2009).
2. C. Clauser, E. Huenges, AGU reference shelf 3. American Geophysical Union 105–126 (1995)
3. F. Birch, Flow of heat in the front range, Bull, Geol. Soc. Am., 61, 567-630 (1950)
4. J.H. sass, C Stone, R.J. Munroe, Volcanol. Geotherm. Res., 20, 145-153 (1984)
5. J.G.M. vamn Mier, M.R.A. van Vliet, K. Wang Tal, Mechanics of Materials 34, 705–724 (2002)
6. A.E. Beck, J. Sci.Instr., 43, 186-189 (1957)
7. H. Hailemariam, F. Wuttke, Heat and Mass Transfer 54, pages1031–1051(2018)
8. K.-H. Bode, Thermal Insulation, 11, 32-52 (1987)
9. Y.A. popov, D. Pribnow, J. Sass, C. Williams, H. Burkhardt, Geothermics, 28, 253-276 (1999)
10. A. Eucken, *d. Phys.* 34 185 (1911)
11. P. Debye, *Ann. Phys.* 39, 789 (1912)
12. D. Bertermann, K. Klug, L. Morper-Buscha, Renew Energy 75:335–347 (2015)